Effect of Sulfuric Acid on the Physiochemical Properties of Chitosan-PVA Blend for Direct Methanol Fuel Cell

RABIRANJAN MURMU[a,b], DEBASHIS ROY[a], HAREKRUSHNA SUTAR[b], PRAGYAN SENAPATI[c], AND SWETAK ABHISEK MOHAPATRA[b]

[a]*Department of Chemical Engineering, Jadavpur University, Kolkata, West Bengal-700032, India.*

[b]*Department of Chemical Engineering, Indira Gandhi Institute of Technology Sarang, Parjang, Dhenkanal-759146, Odisha, India.*

[c]*Department of Mechanical Engineering, Siksha 'O' Anusandhan (Deemed to be University) Bhubaneswar-751030, Odisha, India.*

ABSTRACT

In this work, we have successfully cross-linked the different weight ratio of Chitosan-PVA blend with sulfuric acid. The effect of cross-linker on the properties of blends are studied by using different experimental technique. The cross-linked membrane provides higher ion exchange capacity due to the procurement of extra ionic hooping sites in the membrane. The compatibility of the blends are confirmed from the FTIR and DSC analysis. The crosslinking reaction fastening the phase transition behavior of the blends which reduces the glass transition temperature. The highly compatiblized cross-linked blend provides higher tensile strength and lower modulus at moderate temperature. The significant reduction of weight loss was observed in a cross-linked membrane which enhances thermal stability of the blend. The group which are responsible for higher methanol cross-over are consumed by the cross-linking reaction and a drastic reduction of methanol cross-over was observed. The proton conductivity of the blends are obtained by performing experiment in a four probe impedance analyzer and fitting the EIS data in an equivalent circuit model. At moderate temperature, the cross-linked membrane provides higher proton conductivity than the pure membrane and the proton transport was controlled by Grotthus mechanism. The cross-linked membrane provides higher proton conductivity and membrane selectivity which is beneficial for DMFC design.

KEYWORDS: *Cross-linked Membrane, Storage Modulus, Methanol Cross-over, Proton Conductivity, Membrane Selectivity, DMFC.*

J. Polym. Mater. Vol. **39,** No. 1-2, 2022, 89-109

Correspondence author e-mail:rabiranjan_murmu@rediffmail.com
DOI : https://doi.org/10.32381/JPM.2022.39.1-2.6

1. INTRODUCTION

Fuel cell is considered to be a potential candidate to replace fossil fuel due to their high power density, low toxic emission, simplicity of operation and rapid start-up at room temperature [1-3]. Fuel cell is an excellent electrochemical device which continuously converted chemical energy like hydrogen, methanol to electrical energy with more than 80% efficiency [4, 5]. Recently, direct methanol fuel cell (DMFC) received greater attention for stationary and portable application due to their high power density, cheap price of fuel, high energy density of fuel, simplicity of design and extremely low emission of hazardous pollutant[6-8]. Polymer membrane is the vital component of direct methanol fuel cell which is used as an electrolyte. Currently, Nafion is considered to be a suitable candidate for fuel cell due to its higher proton conductivity and favorable mechanical, thermal and chemical stability. The major drawback of Nafion membrane includes its higher cost, extensive methanol cross-over, poor mechanical and thermal stability at swelling condition which limits the potential application in DMFC. The higher methanol cross-over across the membrane decreases voltage and power density of the DMFC[9-12].

Chitosan and polyvinyl alcohol (PVA) receives greater attention for the development of fuel cell membrane in the past few years due to their favorable properties [13-14]. The chitosan obtained from the shrimp shell are biocompatible, low cost of production, natural abundance and environment friendly [15]. The chitosan based membranes have the ability to reduce methanol cross-over across the membrane which enhances fuel cell performance [16-20]. The PVA membrane gain popularity for DMFC application due to its hydrophilic nature, higher electrochemical selectivity, better mechanical and thermal stability[21-23]. The pristine PVA and chitosan membrane provides poor mechanical and thermal stability due to their higher degree of crystallinity which increases modulus of elasticity. To enhance the physiochemical properties and proton conductivity, both chitosan and PVA are blended together [24-27]. The chitosan-PVA blend provide higher electrochemical selectivity, better mechanical and thermal stability. The blend provides better proton conductivity at lower temperature [28]. However, at lower temperature fuel cell performance was drastically reduces due to the poor management of water which is the biggest issue in fuel cell. To negate the above issue, fuel cell is operated at higher temperature i.e. near to boiling point of water. The state of water i.e. bound water and free water in the membrane plays a significant role for the proton transport and are controlled by Grotthus mechanism [29]. The blend provides poor proton conductivity at higher temperature due to the drastic reduction of free water in the membrane which restricted proton transport by Grotthus mechanism. The bound water content in the membrane plays a significant role for the enhancement of proton conductivity at higher temperature [29]. The bound water content of the composite membranes can be enhanced by cross-linking reaction [30-31]. To enhance the performance of chitosan-PVA blend, cross-linking method is adopted. In this work, we have fabricated the different composition of chitosan-PVA blend and are cross-linked by sulfuric acid. The effect of sulfuric acid on the physiochemical properties of chitosan-PVA blend are studied.

2. EXPERIMENTAL SECTIONS

2.1 Materials and Method

Chitosan from shrimp shell (≥75% deacetylated), Polyvinyl Alcohol Powder (Mw 89000-98000, 98% hydrolyzed), Glacial Acetic acid (>98%), Conc. Sulfuric acid (99%), Methanol (100%) are purchased from Sigma Aldrich, USA. Sodium hydroxide, Hydrochloric acid and Sodium chloride are purchased from Noble Enterprise Berhampur, Odisha. All the chemicals were used without further purification. The deionized and distilled water was produced using a Millipore water purifier, Milli-Q direct water purification system.

2.2 Membrane Preparation

The solution casting method was a conventional approach for the fabrication of polymer membrane and all the composite membranes are prepared by this method. For preparing chitosan-PVA blend, chitosan and PVA solution are prepared separately. For preparing chitosan-PVA blend of 10:90 weight ratio, 4.5g of PVA and 0.5g of chitosan powder are mixed separately with distilled water and glacial acetic acid respectively. The PVA powder was dissolved in a 50 ml distilled water at 65°C for 1hr on magnetic stirrer. Similarly, chitosan solution was prepared by mixing chitosan powder in a 50ml acetic acid (1 vol. %) solution for 1hr on magnetic stirrer followed by sonication. The 1 vol. % acetic acid solution was prepared by mixing 1ml glacial acetic acid with 99ml deionized water. Finally, the both solution were mixed thoroughly on a magnetic stirrer followed by sonication. After mixing, the obtained homogeneous solution was poured in to a flat glass Petri dish and kept it in a hot air over for drying at 35°C and 24 hr. During drying, volatile solvent and moisture was evaporated and a thin sheet of film was obtained. The thin sheet of film was peeled out from the Petri dish and labelled as CP. The similar procedure was followed for the preparation of 20:80 and 30:70 weight ratio of chitosan-PVA blend which were labelled as CP-1 and CP-2 respectively. All the blends are sulfonated by crosslinking with sulfuric acid. For crosslinking, the membrane was dipped in a 2M H_2SO_4 for 24 hr. After 24 hr., the membranes were removed from the sulfuric acid solution and were labelled as CPH, CPH-1 and CPH-2 respectively. The possible reaction scheme of chitosan-PVA blend during membrane synthesis was shown in Figure 1. During mixing, the chitosan and PVA were interacted with the strong intermolecular hydrogen bond which is shown in Figure 1(a). There is also an intramolecular interaction between the ether group and hydroxyl group by strong hydrogen bond in chitosan chain. The chitosan and PVA are interacted with each other by intermolecular linkage and there is no chemical modification of the polymer chain. The chitosan-PVA composite membrane were cross-linked with sulfuric acid. During crosslinking reaction, a new bond was created between the amino group of chitosan and sulfonate group of sulfuric acid which linked the chitosan and sulfuric acid by strong ionic bond. The chemical modification of polymer chain due to the cross-linking reaction is shown in Figure 1(b). When sulfuric acid was added for crosslinking, it produces two ions H^+ and SO_4^{2-}. The amino group present in the chitosan converted to NH_3^+ by protonation of H^+ ion. The NH_3^+ and SO_4^{2-} ions are interacted with each other by strong ionic bond. As the reaction time increases, the membrane was cross-linked by the diffusion of SO_4^{2-} ion between the amino groups and are interacted with each other by strong ionic bond as shown in Figure 1(b).

2.3 Ion Exchange Capacity (IEC) and Water Uptake

The ion exchange capacity (IEC) of the membrane is defined as the amount of ion responsible for proton transport. The amount of ion responsible for proton transport in the membrane is calculated by performing titration test. Before titration, the membrane was dried in a hot air oven for 2hr. at 60°C and placed in the 0.1M HCl solution for 24 hr. After protonation, the H^+ ion (proton) present in the solution was transported to the membrane. The amount of H^+ ion transported to the membrane was measured. For measuring the amount of H^+ ion, the protonated membrane was placed in the 0.1M NaCl solution for 24 hr. to exchange the H^+ ion of the membrane with Na^+ ion of the NaCl solution. After ion exchange, the amount of proton present in the solution was measured by titrating with 0.01M NaOH solution. The IEC of the membrane was calculated by using the following expression.

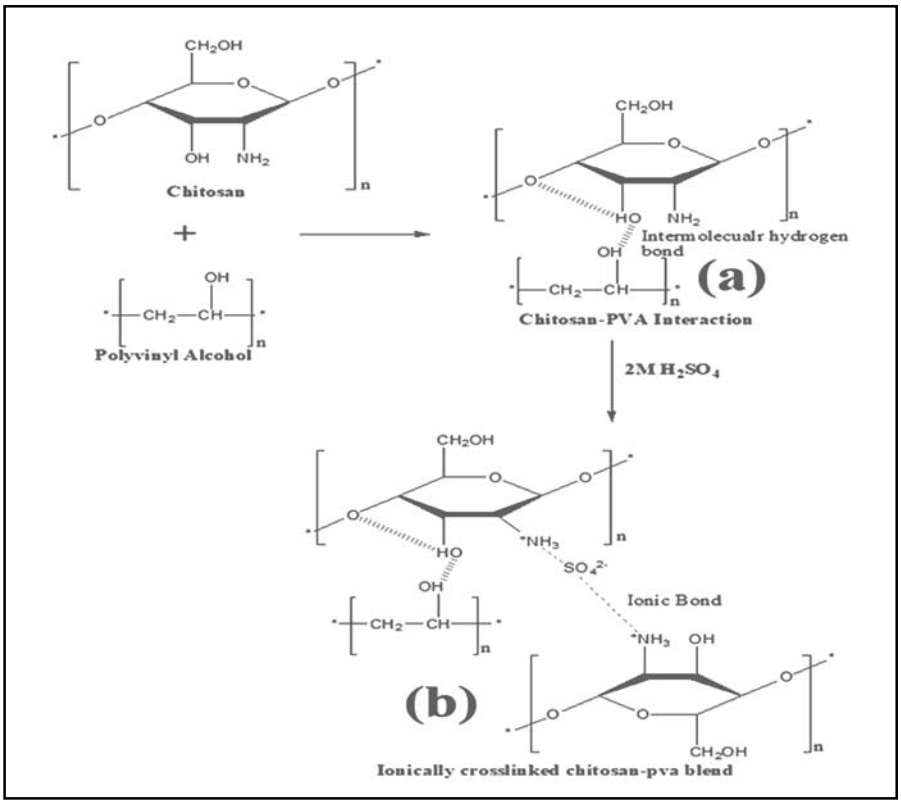

Figure 1: Reaction scheme of chitosan-PVA blend cross-linked with sulfuric acid.

$$IEC\ (meq/g) = \frac{V_{NaOH} \times C_{NaOH}}{W_d} \quad (1)$$

Here V_{NaOH} is the volume of NaOH solution taken for titration, C_{NaOH} is the concentration of NaOH solution, 0.01M and W_d is the dry weight of membrane.

The water uptake capacity (%) of the blend was calculated by measuring dry and wet weight of the membrane. The membrane was dried in a hot air oven for 2 hr. at 60°C and measured its weight, W_d. Then the dry membrane was dipped in a deionized water for 30 hr. and at a particular interval of time, weight of membrane was measured. The above procedure was continued till the membrane achieved an equilibrium water uptake and measured its weight, W_w. The water uptake capacity (%) of the membrane was calculated by using the following equation

$$WU\ (\%) = \frac{W_w - W_d}{W_d} \times 100 = \frac{Change\ in\ weight}{Initial\ dry\ weight} \times 100 \quad (2)$$

Here W_{wet} and W_{dry} are the weight of wet and dry membrane respectively.

2.4 Methanol Permeability

Methanol permeability test for all the fabricated blends was conducted in the glass diffusion cell. The principle for measuring methanol permeability across the membrane in a diffusion cell was reported in our earlier work [32]. During experiment, the methanol permeated across the membrane was collected from the receiver end of diffusion cell and its concentration was measured. The concentration of methanol was measured by measuring its refractive index by SSU Abbe Refractometer (Model No. SSU 58). The methanol

concentration was found from the calibration curve plotted between the refractive index and the concentration of methanol. After measuring the methanol concentration in the receiver end, the methanol permeability across the membrane was calculated by using the following equation

$$P = \frac{C_B(t) V_B L}{A C_A(t_0)} \quad (3)$$

Here P is the methanol cross-over across the membrane in cm^2s^{-1}, C_B (t) and V_B are the methanol concentration at time t and volume of liquid collected from the receiver end respectively. L and A are the thickness and exposed area of the membrane. C_A (t_0) is the initial methanol concentration in compartment A.

2.5 Proton Conductivity

The proton conductivity of the membrane was measured by measuring its membrane bulk resistance (R_b) in four probe impedance analyzer equipped with the temperature sensor. The membrane was interposed between the two SS electrodes which are connected with the external load. The experiment was conducted at different temperature with a frequency range of 0.1-10^6Hz and 0.05V. The bulk resistance, R_b was obtained by fitting the experimental EIS data in an equivalent circuit model. The Randles circuit model is the most appropriate model of the obtained EIS data. From the model parameter, R_b was obtained for all the fabricated membrane. The proton conductivity of the membrane was calculated by using the following equation.

$$\sigma = \frac{L}{R_b A} \quad (4)$$

Here σ is the proton conductivity of the membrane in S/cm, L is the thickness of the membrane, A is the surface area of membrane and R_b is the bulk resistance of the membrane.

3. Membrane Characterization

3.1 Fourier Transform Infrared (FTIR) Analysis

The different function group present in the membrane was confirmed by FTIR peak analyzer (IR-Prestige 21, FTIR spectrometer, M/S Shimadzu Corporation, Japan). For performing test, the dry sample was placed in the sample holder and infrared light was passed with the wavelength range of 400-4000cm^{-1}. The appearance of a strong peak at different wavelength region confirms the present of functional group in the membrane.

3.2 X-ray Diffraction Analysis

The crystalline and amorphous phase of the sample was studied by XRD (Philips, PW1720, USA) machine. The sample was grinded in to power form and placed in the sample holder of XRD machine. The X-ray light generated by Cu-kα radiation at 40kV and 30mA was passed at a scanning rate of diffraction angle (2θ) ranges from 5-85°.

3.3 Differential Scanning Calorimetry (DSC) Analysis

The phase transition behavior and glass transition temperature of the sample was studied by DSC (Perkin-Elmer DSC7, MA, USA). The 5mg of sample was placed in the sample holder and heated from -70-300°C under N_2 atmosphere at a heating rate of 10°C/ min. The experiment was performed with two heating cycle and one cooling cycle at a fixed rate of 10°C/ min.

3.4 Thermo Gravimetric Analysis (TGA)

The thermal degradation behavior of the polymer sample was studied by TGA (Perkin-Elmer TGA, MA, USA). The 5mg of sample was placed in the sample holder and heated from 28-800°C at a fixed heating rate of 10°C/ min under N_2 atmosphere.

3.5 Dynamic Mechanical Analysis

The effect of temperature on the mechanical response of the sample was measured in a DMA (Q800 model, M/S TA instruments, USA). For analysis, the samples were prepared into the dimension of 41×8.5×3mm and tested as per ASTM D5026 standard. The test was conducted at a heating rate of 5°C/minute from 28-300°C under nitrogen atmosphere in a variable frequency mode (oscillatory amplitude of 0.2mm).

3.6 Tensile Test

The tensile strength, strain rate at break and elastic modulus of the polymer sample was measured by UTM (UTM3382, Norwood, MA, USA). Prior to testing, the samples were prepared as per ASTM D638 (Type I, gauge length 50mm). The tensile test was performed at a crosshead speed of 10mm/min at 23°C and 54% humidity.

4. RESULTS AND DISCUSSION

4.1 Fourier Transform Infrared Studies

The chemical structures of the pure and crosslinked chitosan-PVA blend membrane were qualitatively analyzed by FTIR technique and the obtained IR spectra of all the sample is shown in Figure 2. The strong characteristic peak observed at 600cm^{-1} is assigned to C-C bond which signifies the non-compatibility of the blend membrane. There is no peak at 600cm^{-1} for CP membrane which confirms the compatibility of the blend. The strong peak observed at 1100cm^{-1} is assigned to C-O group of chitosan and PVA. The peak intensity of C-O group decreases for CPH membrane due to the crosslinking reaction. The crosslinking reaction depleted the hydroxyl group which reduces peak intensity of C-O group. Furthermore, the amino group (-NH_2) of chitosan was protonated by sulfuric acid during crosslinking reaction. The appearance of a strong peak at 3400cm^{-1} confirms the formation of N^+H bond in CPH membrane. The sulfonate group was interacted with the amino group by a strong ionic bond which can be confirmed by the appearance of a strong peak at 1200cm^{-1} and assigned to O=S=O stretching. The peak intensity of O=S=O stretching in CP membrane was higher than the CP-2 membrane. The amount of sulfonate group interacted in the CP membrane was higher than the CP-2 membrane. The strong peak appeared at 1400 and 2900cm^{-1} for all the membranes are assigned to C-H bending and stretching respectively. The strong peak appeared for all the membrane at 1650cm^{-1} is assigned to N-H bending of the amino group.

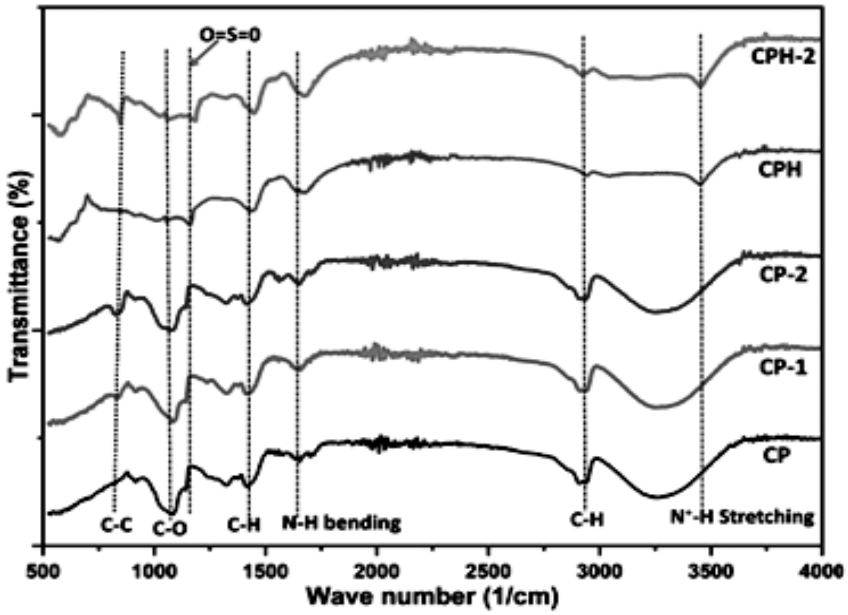

Figure 2. IR spectra of different composite membrane.

4.2 X-ray Diffraction Studies

The amorphous and crystalline phase of the composite membrane was evaluated from the XRD profile. The xrd profile of the different blends are shown in Figure-3. From the XRD profile, the amorphous and crystalline phase are confirmed by the appearance of broad and narrow peak respectively. The peak intensity for the crystalline phase are high as compared to the amorphous phase. The literature reveals that the PVA shows three sharp peak at 10° (002), 19.8° (101) and 28° (200) plane and the chitosan shows a crystalline sharp peak at 10.3° (002), 15.2° (002) and 21.9° (102) [33, 34]. In this work, the sharp peak appeared in the pure chitosan-polyvinyl alcohol blend at 9 & 33° (002), 18° (101) and 28° (200) are assigned to the crystalline phase of polyvinyl alcohol and chitosan. In case of chitosan and polyvinyl alcohol, hydroxyl group and amino group are responsible for the degree of crystallinity. The peak intensity of chitosan-polyvinyl alcohol blend at 9° (002) gradually increases with the decreasing of polyvinyl alcohol (wt. %) in the blend. The reduction of the amount of polyvinyl alcohol in the blend greatly influence the interaction of hydroxyl group present in chitosan and polyvinyl alcohol. All the hydroxyl group are not interacted with each other by hydrogen bond and the unreacted hydroxyl group are responsible for the increment of peak intensity. The amount of unreacted hydroxyl group in the CP-1 and CP-2 membrane are higher which enhances the peak intensity. The crosslinking reaction with sulfuric acid reduces the crystalline phases of the blend. The amino group which is responsible for polymer crystallinity are reacted with sulfonate group and depleted the crystalline domain. The degree of crystallinity of the blend membranes are calculated by using the following expression

$$\chi_c\ (\%) = \frac{A_C}{A_C + A_A} \times 100 \qquad (5)$$

Here, γ_c is the degree of crystallinity of the composite membrane (%), A_C is the area of crystalline phase, A_A is the area of amorphous phase. The degree of crystallinity of the blends are calculated from the peak of XRD profile in origin software and reported in the Table 1. The result indicates that the significant increment of crystalline degree of the blend with the reduction of PVA content. The maximum crystallinity was found in CP-2 membrane followed by CP-1 and CP respectively. The amount of unreacted hydroxyl groups are higher for CP-1 and CP-2 membrane which enhances degree of crystallinity. The compatibility of the CP membrane was confirmed from the IR spectra and the blend contents lower unreacted hydroxyl group. The intermolecular interaction of hydroxyl group in CP blend reduces unreacted hydroxyl group and depleted crystalline phase of the blend. However, a significant increment of hydroxyl group was observed in CP-1 and CP-2 membrane. In case of cross-linked membrane, the CPH membranes has the least degree of crystallinity than CPH-1 and CPH-2 membrane. The amine groups are reacted with sulfuric acid and depleted the crystalline domain. The highest reduction of crystalline degree was observed for CPH membrane followed by CPH-1 and CPH-2 respectively. The amount of sulfonate group reacted in CPH membrane was higher than the CPH-1 and CPH-2 membrane. The amino group responsible for degree of crystallinity in CPH membrane was depleted resulting the enrichment of amorphous phase.

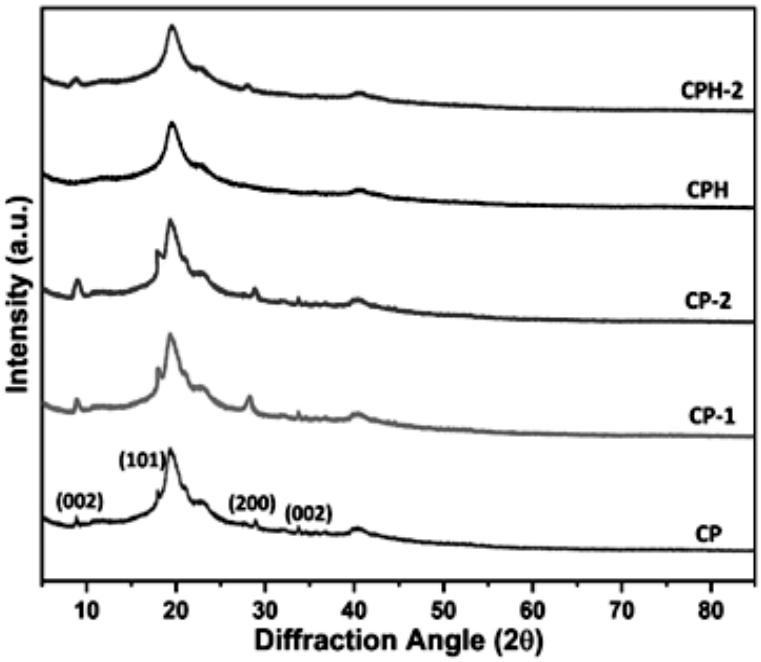

Figure 3: x-ray diffraction plot of the different composite membrane.

4.3 Ion Exchange Capacity and Water Uptake Studies

The water uptake (%) and IEC of the blend membranes are reported in Table-1. The water uptake capacity of the blend increases with the increment of chitosan weight %. The increment of water uptake in the blend was due to the hydrophilic nature of chitosan. The maximum water uptake (%) was found for CP-2 followed by CP-1 and CP respectively. The chemically cross-linked CP membrane provides higher water uptake capacity. The water molecules are bonded with sulfonate group by strong hydrogen bond and thereby increases water uptake capacity. Although the crosslinking reaction reduces free volume and the membrane becomes more dense, compact and tortuous. But the sulfonate group present in the membrane absorb water by chemically bonded with water and increases water uptake capacity. The significant increment of water uptake capacity was observed for cross-linked CP-1 and CP-2 membranes due to their higher incompatibility in structure and the possibility of the higher void volume. The number of water molecules absorbed per the sulfonate group increases due to the presence of more void space in the membrane which eventually increases the water uptake capacity. On the other hand, IEC of the blend membrane decreases with the increment of chitosan weight %. The CP membrane shows higher IEC than CP-1 and CP-2 membrane. The reason for the reduction of IEC in CP-1 and CP-2 membrane was not known. The crosslinking of the blend membrane with sulfuric acid significantly enhances IEC

which was observed in CPH, CPH-1 and CPH-2 membrane. The CPH membrane shows higher IEC than CPH-1 and CPH-2 membrane. During crosslinking reaction, SO_4^{2-} ion diffuses in to the membrane and created an extra ionic sites in the membrane. The creation of an extra ionic sites in a cross-linked membrane is responsible for the enhancement of IEC. The ionic sites in a blend membrane act as a proton transport channel. Moreover, the protonation of amine group in the cross-linked blend enhances ion exchange capacity. The amount of SO_4^{2-} ions diffuses in the CP membrane was higher than the CP-1 and CP-2 membrane. Hence, the CPH membrane provides higher IEC than CPH-1 and CPH-2 membrane.

TABLE 1: Physiochemical properties of the composite membranes at room temperature.

Samples	Water Uptake (%)	IEC (meq/g)	χ_c (%)	Tensile Strength (MPa)	Elastic Modulus (MPa)	Methanol Permeability, $P \times 10^{-7}$ (cm^2/sec.)
CP	133	0.575	15.46	42.08	1379.41	2.42
CP-1	136	0.413	18.24	38.73	1250.23	3.18
CP-2	145	0.328	22.34	20.41	402.46	4.67
CPH	138	0.832	8.32	46.12	448.44	0.34
CPH-1	147	0.71	12.46	41.28	387.19	1.46
CPH-2	154	0.64	17.38	23.82	405.44	1.74

4.4 Thermal Property Studies

The effect of temperature on the phase transition behavior of composite membranes are studied from the DSC heating scan. The glass transition temperature and melting temperature of the composite membranes are obtained from the endothermic peak of heating curve. The DSC heating curve of the different blends are shown in Figure 4. The summary of the DSC profile are tabulated in the Table 2. In the table, T_{g1}: glass transition temperature of PVA in the blend, T_{g2}: glass transition temperature of the chitosan (in case non-compatible blend) and blend (in case of compatible blend). The two stages of phase relaxation was observed for non-compatible blend. The two stages of phase transition was observed in CP-1 and CP-2 blend which signifies the non-compatibility of the blend. The appearance of two endothermic peak signifies the glass transition temperature of the blend species. The first and second peak corresponds to the glass transition temperature of polyvinyl alcohol and chitosan. But in the case of CP membrane, only one phase transition was observed and the first endothermic peak corresponds to glass transition temperature of the blend. All the membrane shows a sharp endothermic peak at higher temperature which corresponds to melting temperature. The CP membrane shows lower glass transition temperature than CP-1 and CP-2 membrane. The well suited firmly interacted CP blend has lower crystalline domain than CP-1 and CP-2 membrane and the polymer chains are move freely. But in case

of CP-1 and CP-2 membrane, the mobility of polymer chains are restricted by the crystalline domain which delays phase transition from glassy to rubbery state. However the crosslinking reaction significantly reduces glass transition temperature of the blend and the CPH membrane provides lower glass transition temperature. The crystalline domains are depleted which fastening the mobility of the polymer chain. The melting temperature of the CP membrane was higher than the CP-1 and CP-2 membrane. The chitosan and polyvinyl alcohol are firmly interacted with each other which delays the melting of blend. On the other hand if the membrane was cross-linked with sulfuric acid, the melting temperature decreases. At higher temperature the sulfonate ion in the blend catalyzed the

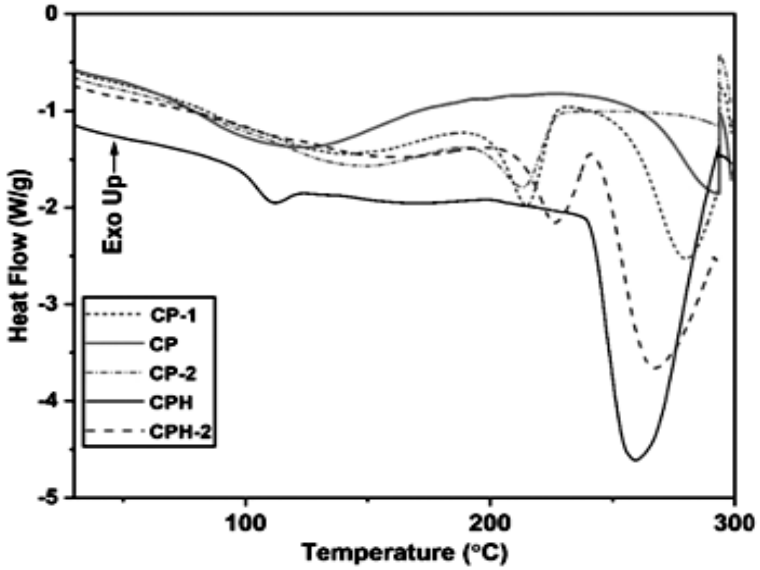

Figure 4: The reheating curve of the different composite membrane obtained from the DSC scan.

oxidation reaction which degraded the polymer backbone.

The thermal stability of the polymer blend are studied by TGA thermograph. The weight loss curve of the different polymer blends are shown in Figure 5. From the TGA curve, the three stages of weight loss was observed for all the membrane. The first stage of weight loss was observed in the range of 80-200°C. The main weight loss was occurred due to the evaporation of loosely attached volatile solvent and water. The solvent used for the fabrication of polymer blend was glacial acetic acid (boiling point: 118°C) which evaporated in this stage. The weight loss curve of all the polymer membranes are similar during the first stage of weight loss. There was slight increment of weight loss in CP-1 and CP-2 membrane due to the higher loss of carbon in the polymer backbone. The loss of carbon atom was due to the

incompatible structure of the blend resulting the weak interaction of polymer chain. The carbon atom are detached from the loosely attached chain even at lower temperature. When the polymer blends are cross-linked with sulfuric acid, the thermal stability of the membrane was enhanced by the strong intermolecular linkage which suppress the loss of carbon atom. The weight loss was occurred due to the loss of volatile solvent and water only. The water molecules are strongly attached with the sulfonate group which delays the evaporation loss of water. Hence, lower weight loss was observed in the cross-linked membrane. The second weight loss stage for all the membrane was observed in the range of 200-400°C. The polymer membrane were degraded due to the thermal oxidation of oxygen function group and thermal desulfonation of sulfonate group. The desulfonation of the sulfonate group was occurred in the cross-linked membrane on the temperature range of 300-400°C. The presence of sulfonate group in the cross-linked membrane delays the degradation of polymer chain. The weight loss due to the thermal oxidation of oxygen function group was occurred in the range of 200-300°C for all the membrane. In case of pure blend, the maximum weight loss was observed in CP blend followed by CP-2 and CP-1 blends. The residual bound water was evaporated during this stage. The reason for higher weight loss in a compatibilized CP blend is clearly not known. It may be due to the presence of higher residual bound water which evaporated during this stage. Moreover, the carbon atoms are detached from the polymer chain which resulted

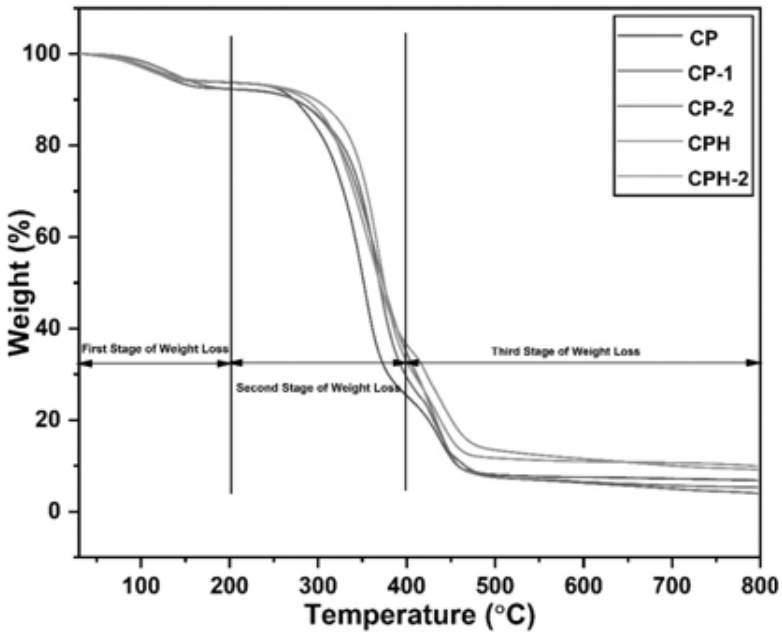

Figure 5. The weight loss curve of the blends obtained from the TGA.

higher weight loss. The cross-linked membrane provides higher thermal stability at the temperature range of 200-300°C. The bound water was strongly interacted with the sulfonate group and prevents the evaporation loss of water. But when the temperature exceed 300°C, sulfonate group catalyzed the oxidation reaction and the polymer chain degraded faster. During this temperature range, higher weight loss was observed in the cross-linked membrane. The third weight loss stage was observed in the temperature range of 450-800°C. During third stage of weight loss, polymer backbones are degraded. The cross-linked membrane shows higher thermal stability than the pristine membrane.

TABLE 2: The summary of the DSC and TGA data of different blends.

Sample Code	$T_{g,1}$(°C)	$T_{g,2}$ (°C)	T_m (°C)	TGA profile data			
				1st stage of weight loss at 200°C (%)	2nd stage of weight loss between 200-400°C (%)	3rd stage of weight loss at 450°C (%)	Final Residue 790°C (%)
CP	—-	120.57	280.17	6.29	68.36	88.18	6.87
CP-1	136.05	—-	286.76	7.66	57.64	87.59	5.33
CP-2	143.18	—-	293.57	7.82	62.8	87.32	4.08
CPH	—-	110.82	259.97	6.14	61.03	84.02	10.03
CPH-1	132.72	—-	263.42	6.18	59.61	81.72	9.84
CPH-2	137.40	—-	265.27	6.21	57.28	79.75	9.22

4.5 Mechanical Property Studies

The effect of temperature on the mechanical response of the polymer blend was studied by DMA and the response curve was plotted in Figure 6. The response of storage modulus with the temperature is shown in Figure 6(a). The storage modulus of CP membrane was higher than the CP-1 and CP-2 membrane. The modulus response was gradually changes with the temperature. The compatibility structure and degree of crystallinity of the polymer blend plays a significant effect on the modulus of the membrane. At 100°C, the highly compatitilized CP blend provides lower storage modulus than the CP-1 and CP-2 blend. The higher temperature enhances the mobility of the chain thereby fastening the phase transition behavior. However, the phase transition behavior was lower for non-compatible CP-1 and CP-2 blend. The two distinct immiscible phase with higher crystalline domain delays the phase transition from glassy to rubbery phase. The compatible structure and lower degree of crystallinity of the CP membrane enhances the mobility of the chain. The mobility of the chain enhances chain flexibility and reduces storage modulus. The crosslinking reaction reduces the degree of crystallinity of the membrane and the membrane becomes more flexible. The

depletion of crystalline degree in the blend enhances the mobility of the chain which fastening the phase transition. For the cross-linked membrane, the maximum modulus was observed in CPH-2 membrane. The storage modulus of CPH membrane was lower due to its depleted crystalline domain. The response of tan δ with temperature for all the polymer membranes are shown in Figure 6(b). The glass transition temperature of the polymer membranes are obtained from the peak of the tan δ curve. The two stage phase relaxation was observed in CP-1 and CP-2 blend due to non-compatible structure. The similar behavior was also observed in the DSC heating scan. During phase relaxation, the first and second peak corresponds to the glass transition temperature of chitosan and the polyvinyl alcohol respectively. But in case CP blend, it shows one stage phase transition relaxation and the peak corresponds to the glass transition temperature of the blend. The glass transition temperature of the CP blend was lower than the second stage glass transition temperature of the CP-1 and CP-2 blend which

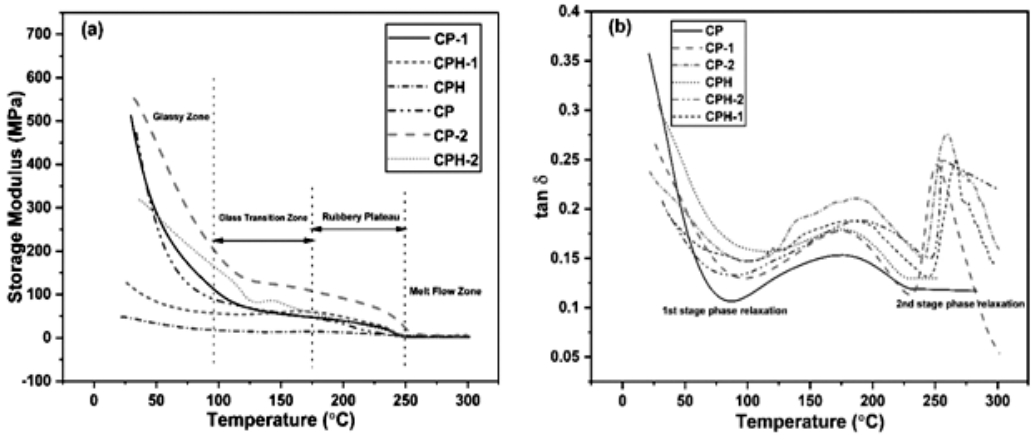

Figure 6. The effect of temperature on the mechanical response of blends (a) The effect on storage modulus curve (b) The response of tan δ curve.

signifies the flexibility of the blend. The glass transition temperature range of the polymer membranes are similar with the DSC scan.

The elastic modulus of all the polymer membranes are obtained from the slope of stress-strain curve and reported in Table 1. The linear portion of the stress-strain curve was considered for obtaining the slope. The elastic modulus of the polymer blend increases with the increment of chitosan wt. % in the blend. The maximum modulus was found for CP membrane followed by CP-1 and CP-2 membrane respectively. The entanglement of polymer chain in the compatibilized blend restrict the mobility of chain at lower temperature. Hence the highly compatible CP blend provides higher storage modulus than the non-compatible blend. Although the CP membrane provides higher modulus but it also

breaks at higher strain which is beneficial for practical application. The strong interaction of the polymer chain as well as its lower crystalline degree enhances the flexibility of the blend and the membrane breaks at higher strain. The CP blend are much more flexible and ductile than the CP-1 and CP-2 membrane. The crosslinking reaction reduces the elastic modulus of the membrane by reducing crystalline degree and the membrane breaks at higher strain. The membrane becomes more flexible and ductile. The tensile strength of all the polymer membranes are obtained from the stress-strain curve and reported in Table-1. The maximum tensile strength was found for CP membrane followed by CP-1 and CP-2 membrane. The polymer chain are strongly interacted in CP blend which resulted higher tensile strength. After crosslinking, the tensile strength of the blend increases and the CPH membrane provides maximum strength among the cross-linked membrane. After crosslinking reaction, the tensile strength of the CP blend was increased from 42.08MPa to 46.12MPa. The SO_4^{2-} ion of the sulfuric acid strongly linked the polymer chain via ionic bond thereby enhancing strength of the blends. Moreover, the crosslinking reaction reduces modulus of the blend by consuming crystalline group of the blend. The polymer chain becomes flexible and breaks at higher strain. The higher tensile strength and lower modulus are the favorable properties of electrolyte membrane for DMFC design.

4.6 Methanol Cross-over Studies

The methanol cross-over across the polymer membrane was measured in a glass diffusion cell using equation (4) and reported in the Table 1. The test was conducted in a diffusion cell for 2M methanol feed. The test result indicates the reduction of methanol cross-over with the increment of polyvinyl alcohol in the blend. The CP membrane provides least methanol cross-over among the pure fabricated blend. The CP membrane was highly compatible than the CP-1 and CP-2 membrane. The amount of free hydroxyl group in the CP membrane was lower than the CP-1 and CP-2 membrane. The depletion of hydroxyl group with the increment of polyvinyl alcohol in the blend are confirmed from IR analysis. The amount of free hydroxyl group present in the membranes are responsible for methanol cross-over. The methanol reacted with the hydroxyl group of chitosan and PVA in the membrane to form a strong hydrogen bond[19]. Hence the CP membrane provides excellent methanol blocking ability than the CP-1 and CP-2 membrane. The methanol cross-over for the highly compatible CP membrane is 2.42×10^{-7} cm^2/sec. The methanol cross-over for the CP membrane is good agreement with the earlier report[19, 30 &31]. The crosslinking reaction with sulfuric acid further reduces the methanol cross-over. The free hydroxyl group present in the polymer chain are consumed due to the reaction with sulfonate group. The polymer chains are linked with each other by strong ionic bonds and the membrane becomes more compact and tortuous. There is a lack of void space available for the transport of methanol which reduces methanol cross-over. The methanol cross-over for CPH membrane was 0.34×10^{-7} cm^2/sec, which is least among the other cross-linked membrane. The methanol cross-over of CPH membrane was lower than the commercial

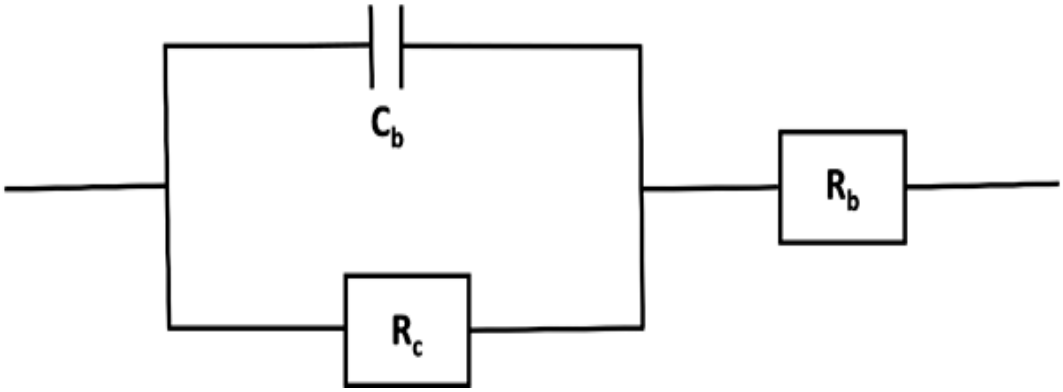

Figure 7: The equivalent CPE based Randles circuit model for fitting the EIS data and obtaining the membrane bulk resistance, R_b in Ω.

N117 membrane [19, 35]. The methanol cross-over data for CP was quite similar with the highly effective N212-GO membrane reported by Bong Gill Choi et al., [36].

4.7 Ionic Conductivity Studies

Randles circuit model parameter: The electrolyte or membrane bulk resistance is represented by R_b in Ω. The bulk resistance was obtained by fitting the EIS data in the model. The R_c is the electrode or contact resistance in Ω and the constant phase element (CPE) of the model is represented by C_b which is suitable for capacitor in the experiment. The bulk resistance plays a significant role for the enhancement of fuel cell performance. The reduction of bulk resistance increases the open circuit voltage of the fuel cell which increases power density.

The membrane bulk resistance of all the polymer membranes are obtained from the equivalent randles circuit model and the proton conductivity was calculated using equation (4). The values of membrane bulk resistance and proton conductivity for all the composite membranes are reported in the Table 3. The electrolyte resistance increases in the membrane when the composition of the polyvinyl alcohol in the blend decreases. The maximum proton transport resistance was found in CP-2 membrane followed by CP-1 and CP membrane respectively. The weight percentage of chitosan and polyvinyl alcohol in the polymer blend plays a significant role for the proton conductivity. The highly compatible CP blend offers high proton conductivity due to the reduction of bulk resistance and its higher IEC. The proton conductivity of the blend reduces with the increment of chitosan in the blend which was observed for CP-1 and CP-2 membrane. The proton conductivity values of all the membranes are reported at 28°C and 70°C. The effect of temperature on the proton conductivity of blend is shown in Fig. 8(a). The proton conductivity of the cross-linked membrane was far higher than the pristine membrane. The crosslinking reaction enhances

the proton transport site in the membrane which increases the proton conductivity. The proton is transported through the electrolyte membrane by two key mechanism (i) Grotthus (ii) vehicular mechanism[37]. Generally, proton transported by Grotthus mechanism provides higher proton conductivity. In Grotthus mechanism, protons are conducted at hydrated condition by combination with free water to from hydronium ion. At low temperature, IEC and the free water content in the membrane plays a significant effect on proton conductivity [38]. Due to the presence of free water, the rate of proton transport through the membrane was regulated by Grotthus mechanism. At higher temperature, 70°C and low humidity condition, proton transport through the membrane was controlled by vehicular mechanism. Due to the lack of free water, water molecules will come together to form water cluster which act as a vehicle for proton transport. The proton transport by vehicular mechanism is lower than the Grotthus mechanism. For that reason, the pristine chitosan-PVA blend provides lower proton conductivity. But in case of cross-linked membrane, the sulfonate group creates a strong bonding with water and the water molecules will not escape easily even at boiling temperature of water. The presence of water in the polymer chain facilitates proton transport by Grotthus mechanism. The proton was transported through the membrane by the combined effect of Grotthus and vehicular mechanism. Moreover, the addition of sulfonate group protonated amine group thereby enhancing the proton transport channel in the membrane. Hence the proton conductivity of cross-linked blend is higher than pure blend. The maximum proton conductivity was found for CPH membrane. For cross-linked membrane, temperature plays a significant role for the enhancement of proton conductivity. For CPH membrane. The threefold increase of the proton conductivity was observed with the increment of temperature from 28 to 70°C. The increment of temperature enhances the mobility of the proton which increases proton conductivity.

TABLE 3: Membrane resistance (R_b) and Proton conductivity (σ) of the composite membranes obtained at room temperature (28°C) and 70°C.

Sample Code	Membrane Resistance, R_b (Ω)		Proton Conductivity, σ (Scm^{-1}) $\times 10^{-3}$	
	28°C	70°C	28°C	70°C
CP	278.51	226.29	0.13	0.16
CP-1	402.29	329.15	0.09	0.11
CP-2	905.17	517.24	0.04	0.07
CPH	32.32	26.23	1.12	1.38
CPH-1	53.24	38.93	0.68	0.93
CPH-2	77.03	51.72	0.47	0.70

The activation energy required for proton

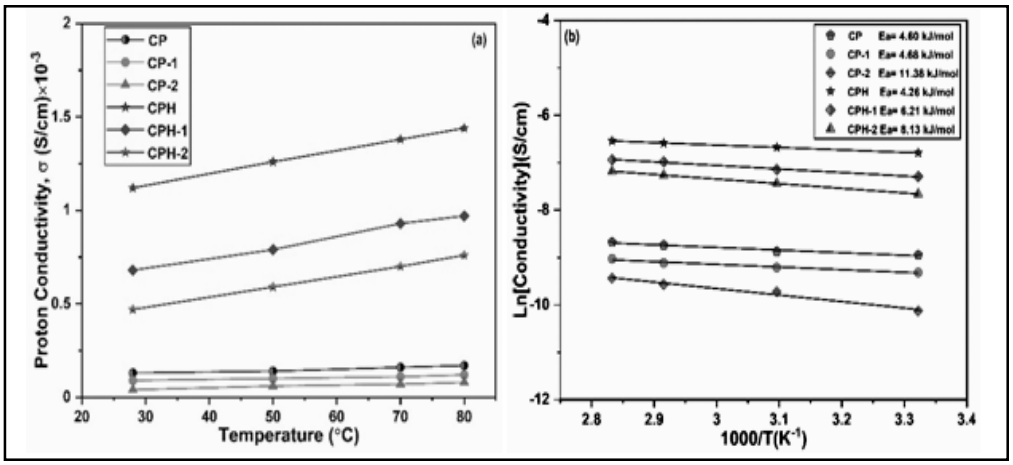

Figure 8. (a) The variation of the proton conductivity of blends with temperature (b) The Arrhenius plot for the evaluation of activation energy.

transport in the composite membrane was obtained from the relationship between the proton conductivity and temperature. The temperature dependency on the mobility of proton transport is expressed in the form of Arrhenius equation. The Arrhenius equation for evaluating activation energy is represented in the following expression

$$\ln [\sigma] = \ln [\sigma_0] - \frac{Ea}{RT} \qquad (7)$$

Here, σ and σ_0 are the proton conductivity and pre-exponential factor of membrane respectively, in S cm^{-1}, Ea is the activation energy required for proton transport in kJ/mol., R is the universal gas constant (8.314 J/mol. K) and T is the absolute temperature in K. The activation energy of the composite membranes were evaluated from the slope of the curve plotted between ln σ vs 1000/T. The Arrhenius plot for the proton conductivity data is shown in Fig. 8(b). The proton conductivity data points are fitted with linear fitting in origin software and the activation energy was obtained from the slope of the curve. The activation energy of all the membranes are evaluated to predict the effect of temperature on the mobility of proton transport. From the slope of the Arrhenius plot, activation energy of the membranes are obtained in the range of 4.26-11.38 kJ/mol. The activation energy reported for the commercial membrane N112 and N117 are 10.39 and 7.46 kJ/mol. respectively[30, 39]. The activation energy reported for CP membrane was quite lower than the CP-1 and CP-2 membrane. It signifies the dependency of temperature on the mobility of proton transport with the enhancement of chitosan in the blend. The degree of incompatibility increases the activation energy of the blend and temperature plays a significant role on the mobility of proton transport. On the other hand there was a least effect of temperature on the mobility of proton transport in highly compatible CP membrane. Furthermore the crosslinking reaction significantly reduces the activation energy of the blend which was observed in CPH and CPH-2 membrane. This indicates that the crosslinking reaction alleviating the mobility of

proton transport in the polymer channel. The activation energy reported for CPH membrane, 4.16 kJ/mol. is lower than the CPH-2 membrane, 8.13 kJ/mol. On the other hand, the activation energy of CP-2 membrane upon crosslinking shows contrasting trend. After crosslinking, the activation energy increases from 4.68 kJ/mol. for pure CP-1 membrane to 6.21kJ/mol. for CPH-1 membrane. The reason for the increment of activation energy in the membrane was quite unclear and may be the possibility of the lack of chemical reaction on the blend during crosslinking reaction with sulfuric acid. The increment of activation energy in the membrane decreases proton conductivity at lower temperature. The mobility of the proton transport was suppressed by the lack of sulfonic group on the polymer channel which depleted the proton transport channel.

The membrane selectivity (S) of the composite membrane was calculated from the relationship between proton conductivity and methanol permeability. The general expression for calculating membrane selectivity is given below

$$S\ (S.sec./cm^3) = \frac{Proton\ Conductivity, \sigma}{Methanol\ Permeability, P} \quad (8)$$

The membrane selectivity of the different composite membranes are obtained at room temperature and reported in the Table 4. For the pure blend, CP membrane provides higher membrane selectivity than CP-1 and CP-2 membrane. The methanol cross-over across the membrane greatly influenced the membrane selectivity. The CP membrane provides favorable proton conductivity and lower methanol permeability. After crosslinking reaction with sulfuric acid a significant improvement of membrane selectivity was observed in the membrane. The crosslinking reaction not only increases proton conductivity but also blocking the transport of methanol through the polymer channel. It was observed that the crosslinking reaction of CP membrane increases the membrane selectivity form

TABLE 4: The ionic conductivity (σ), methanol permeability (P) and membrane selectivity (S) values for the polymer electrolyte membrane obtained at room temperature (28°C).

Sample Code	Proton Conductivity, σ (S/cm)×10^{-3}	Methanol Permeability, P (cm^2/sec.)×10^{-7}	Membrane Selectivity, S (S.sec./cm^3)×10^3
CP	0.13	2.42	0.54
CP-1	0.09	3.18	0.28
CP-2	0.011	4.67	0.024
CPH	1.12	0.34	32.94
CPH-1	0.68	1.46	4.65
CPH-2	0.47	1.74	2.71
N117[19]	71	5.2	139.2
N212-GO[36]	40	0.792	50.51

0.54×10^3 to 32×10^3 S.sec./cm^3. Although the reported values are far lower than the commercial N117 and N212-GO membrane but it is encouraging for the further development. The cross-linked membrane provides higher membrane selectivity which is beneficial for direct methanol fuel cell design.

CONCLUSION

The weight ratio of chitosan and polyvinyl alcohol in the blend significantly affects its physiochemical properties. The incompatible blend shows dual stage phase relaxation during phase transition and also provides higher glass transition temperature. The crosslinking reaction depleted the crystalline degree of all the blends which fastening the phase transition from glassy to rubbery state and reduces glass transition temperature. The cross-linked membrane shows excellent thermal stability up to 450°C due to the strong intermolecular ionic bond. But when the temperature exceed 450°C, sulfonic acid catalyzed oxidation reaction which degraded the polymer chain faster. The cross-linked membrane provides higher tensile strength and lower storage modulus which are favorable properties of fuel cell membrane. The crosslinking reaction alleviating the mobility of proton transport and the activation energy of highly performed CPH blend (4.16 kJ/mol.) is quite lower than the N117 membrane. The protonation of amine group enhances ionic conductivity in a cross-linked blend. At 70°C, the CPH membrane provides superior proton conductivity, 1.38×10^{-3} S/cm. The crosslinking reaction prevents the loss of water at 70°C and the proton transport was controlled by both Grotthus and vehicular mechanism. The reduction of methanol cross-over across the cross-linked membrane enhances membrane selectivity. The cross-linked membrane provides lower methanol permeability and excellent proton conductivity which is beneficial for direct methanol fuel cell design.

REFERENCES

1. B. L. Yi (2003) Fuel Cell- Principle Technology Application; Chemical Industry Press: Beijing, China.
2. A. Chandan, M. Hattenberger, A. El-kharouf (2013). High temperature polymer electrolyte membrane fuel cells (PEMFC)-A review, *Journal of Power Sources,* 231: 264-278.
3. B. C. H. Steele and A. Heinzel (2001). Materials for fuel-cell technologies. *Nature,* 414: 345-352.
4. D. W. Shin, M. D. Guiver, Y. M. Lee (2017). Hydrocarbon-based polymer electrolyte membranes: Importance of morphology on ion transport and membrane stability, *Chemical Reviews,* 117: 4759-4805.
5. Y. J. Wang, J. Qiao, R. Baker, J. Zhang (2013). Alkaline polymer electrolyte membranes for fuel cell applications, *Chemical Society Reviews,* 42: 5768-5787.
6. J. Divisek, J. Fubrmann, K. Gartner and R. Jung (2003). Environmental aspects of direct methanol fuel cell: Experimental detection of methanol electro-oxidation product, *Journal of Electrochemical Sources,* 150: A811-A825.
7. N. W. Deluca, Y. A. Elabd (2006). Polymer electrolyte membranes for the direct methanol fuel cell: a review, *Journal of Polymer Science Part B-Polymer Physics,* 44: 2201-2225.
8. J. H. Wee (2006). Which type of fuel cell is more competitive for portable application: direct methanol fuel cells or direct borohydride fuel cells, *Journal of Power Sources,* 161: 1-10.

9. Mohammad A. Barique, Eiji Tsuchida, Akihiro Ohira and Kohji Tashiro (2018). Effect of Elevated Temperatures on the States of Water and Their Correlation with the Proton Conductivity of Nafion, *ACS Omega,* 3: 349-60.

10. K. Scott, W. Taama and J. Cruickshank (1997). Performance and modeling of a direct methanol solid polymer electrolyte fuel cell, *Journal of Power Sources,* 65: 159-171.

11. G. Murgia, L. Pisani, A. K. Shukla, K. Scott (2003). A numerical model of a liquid–feed solid polymer electrolyte DMFC and its experimental validation, *Journal of Electro-chemical Society,* 150: A1231-A1245.

12. B. Y. Wang, L. D. Hun, N. Y. Liu, K. P. O. Mahesh, S. J. Lue (2013). Cell performance modeling of direct methanol fuel cells using proton-exchange solid electrolytes: Effective reactant diffusion coefficients in porous diffusion layers, *Journal of Power Sources,* 22: 275-283.

13. Hong Wu, Bin Zheng, Xiaohong Zheng, Jingtao Wang, Weikang Yuan, Zhongyi Jiang (2007). Surface-modified Y zeolite-filled chitosan membrane for direct methanol fuel cell, *Journal of Power Sources,* 173: 842-852.

14. C. C. Yang, Y. J. Lee, M. J. Yang (2009). Direct methanol fuel cell (DMFC) based on PVA/MMT composite polymer membranes, *Journal of Power Sources,* 188(1): 30-37.

15. J. Ma & Y. Sahai (2013). Chitosan biopolymer for fuel cell applications. *Carbohydrate Polymers,* 92(2): 955-975.

16. Jie Wang, Chunli Gong, Sheng Wen, Hai Liu, Caiqin Qin, Chuanxi Xiong, Lijie Dong (2018) Proton exchange membrane based on chitosan and solvent-free carbon nanotube fluids for fuel cells applications, *Carbohydrate Polymers,* 186: 200-207.

17. Jin Ah Seo, Joo Hwan Koh, Dong Kyu Roh, Jong Hak Kim (2009). Preparation and characterization of crosslinked proton conducting membranes based on chitosan and PSSA-MA copolymer, *Solid State Ionics,* 180: 998-1002.

18. Yan Xiang, Meng Yang, Zhibin Guo, Zheng Cui (2009). Alternatively chitosan sulfate blending membrane as methanol-blocking polymer electrolyte membrane for direct methanol fuel cell, *Journal of Membrane Science,* 337: 318-323.

19. S. Meenakshi, S. D. Bhat, A. K. Sahu, P. Sridhar, S. Pitchumani, A. K. Shukla (2012). Chitosan-Polyvinyl Alcohol-Sulfonated Polyethersulfone Mixed-Matrix Membranes as Methanol-Barrier Electrolytes for DMFCs, *Journal of Applied Polymer Science,* 124, E73-E82. DOI: https://doi.org/10.1002/app.35522

20. R Murmu, D. Roy, S. Jena, H. Sutar (2022) Development of Chitosan based hybrid membrane modified with Ionic-Liquid and Carbon Nanotubes for direct methanol fuel cell operating at moderate temperature, *Polymer Bulletin,* 2022. DOI: https://doi.org/10.1007/s00289-022-04246-7

21. J. W. Rhim, H. B. Park, C. S. Lee, J. H. Jun, D. S. Kim, Y. M. Lee (2004). Cross-linked polyvinyl alcohol membranes containing sulfonic acid group: proton and methanol transport through membranes, *Journal of Membrane Science,* 238: 143-151.

22. D. S. Kim, H. B. Park, J. W. Rhim, Y. M. Lee (2004). Preparation and characterization of cross-linked PVA/SiO_2 hybrid membranes containing sulfonic acid groups for direct methanol fuel cell applications, *Journal of Membrane Science,* 240: 37.

23. C. W. Lin, Y. F. Huang, A. M. Kannan (2007). Cross-linked polyvinyl alcohol and poly (styrene sulfonic acid-co-maleic anhydride) based semi-interpenetrating network as proton conducting membranes for direct methanol fuel cells, *Journal of Power Sources,* 171: 340-347.

24. A. S. Ariyaskul, R. Y. Huang, P. L. Douglas, R. Pal, X. Feng, P. Chen, L. Liu (2006). Blended chitosan and polyvinyl alcohol membranes for the pervaporation dehydration of isopropanol, *Journal of Membrane Science,* 280: 815-823.

25. Y. S. Zhou, D. Z. Yang, X. M. Chen, Q. Xu, F. M. Lu, J. Nie (2008). Electrospun water soluble carboxyethyl chitosan/polyvinyl alcohol nanofibrous membrane as potential wound dressing for skin regeneration, *Biomacromolecules,* 9: 349-54, 2008.

26. J. M. Yang, W. Y. Su, T. L. Leu, M. C. Wang (2004). Evaluation of chitosan/PVA blended hydrogel membranes, *Journal of Membrane Science,* 236, 39.

27. L. G. Wu, C. L. Zhu, M. Liu (1994). Study of a new pervaporation membrane Part I. Preparation and characteristics of the new membrane, *Journal Membrane Science,* 90: 199-205.

28. LY. F. Lin, C. Y. Yen, C. H. Hung, Y. H. Hsiao, C. C. M. Ma (2007). A novel blends based on sulfonated montmorillonite modified Nafion®for DMFCs. *Journal of Power Sources,* 168: 162-166.

29. R. Murmu, H. Sutar (2018). A Novel SPEEK-PVA-TiO_2 Proton Conducting Composite Membrane for PEMFC operations at Elevated Temperature, *Journal of Polymer Materials,* 35(4): 409-431, 2018.

30. Panu Danwanichakul and Pongchayont Sirikhajornnam (2013). An Investigation of Chitosan-Grafted-Poly (vinyl alcohol) as an Electrolyte Membrane, *Journal of Chemistry,* Article ID: 642871. DOI: https://doi.org/10.1155/2013/642871

31. Jen Ming Yang and Hsien Chih Chiu (2012). Preparation and characterization of polyvinyl alcohol/chitosan blended membrane for alkaline direct methanol fuel cells, *Journal of Membrane Science,* 419-420, 65-71.

32. R Murmu, D Roy, S. C. Patra, H Sutar, P Senapati (2022). Preparation and characterization of the SPEEK/PVA/Silica hybrid membrane for direct methanol fuel cell (DMFC), *Polymer Bulletin,* 79: 2061-2087.

33. K Nakane, T Yamashita, K Iwakura, F Suzuki (1999). Properties and structure of poly(vinyl alcohol)/silica composites, *Journal of Applied Polymer Science,* 74(1): 133-138.

34. Yuanyuan Zhang, Xiaobo Huang, Bin Duan, Lili Wu, Shuo Li, Xiaoyan Yuan (2007). Preparation of electrospun chitosan/poly(vinyl alcohol) membranes, *Colloid and Polymer Science,* 285: 855-863.

35. Y Chun-Chen and L Ying-Jeng (2009). Preparation of the acidic PVA/MMT nanocomposite polymer membrane for the direct methanol fuel cell (DMFC), *Thin Solid Films,* 517:4735-4740.

36. Bong Gill Choi, Yun Suk Huh, Young Chul Park, D. Hwan Jung, Won Hi Hong, Ho Seok Park (2012). Enhanced transport properties in polymer electrolyte composite membranes with graphene oxide sheets, *Carbon,* 50:5395-5402.

37. Dae Sik Kim, Ho Bum Park, Ji Won Rhim, Young Moo Lee (2005). Proton conductivity and methanol transport behavior of cross-linked PVA/PAA/silica hybrid membranes, *Solid State Ionics,* 176: 117-126.

38. R Murmu and H Sutar (2018). Steady state analysis of water transport through sulfonated poly ether ether ketone (SPEEK) membrane for fuel cell application, *Journal of Polymer Materials,* 35(1): 103-118.

39. Arindam K. Das, Murli Manohar and Vinod K. Shahi (2018). Cation-Exchange Membrane with Low Frictional Coefficient and High Limiting Current Density for Energy-Efficient Water Desalination, ACS Omega, 3: 10331-10340.

Received: 13-05-2022

Accepted: 04-06-2022